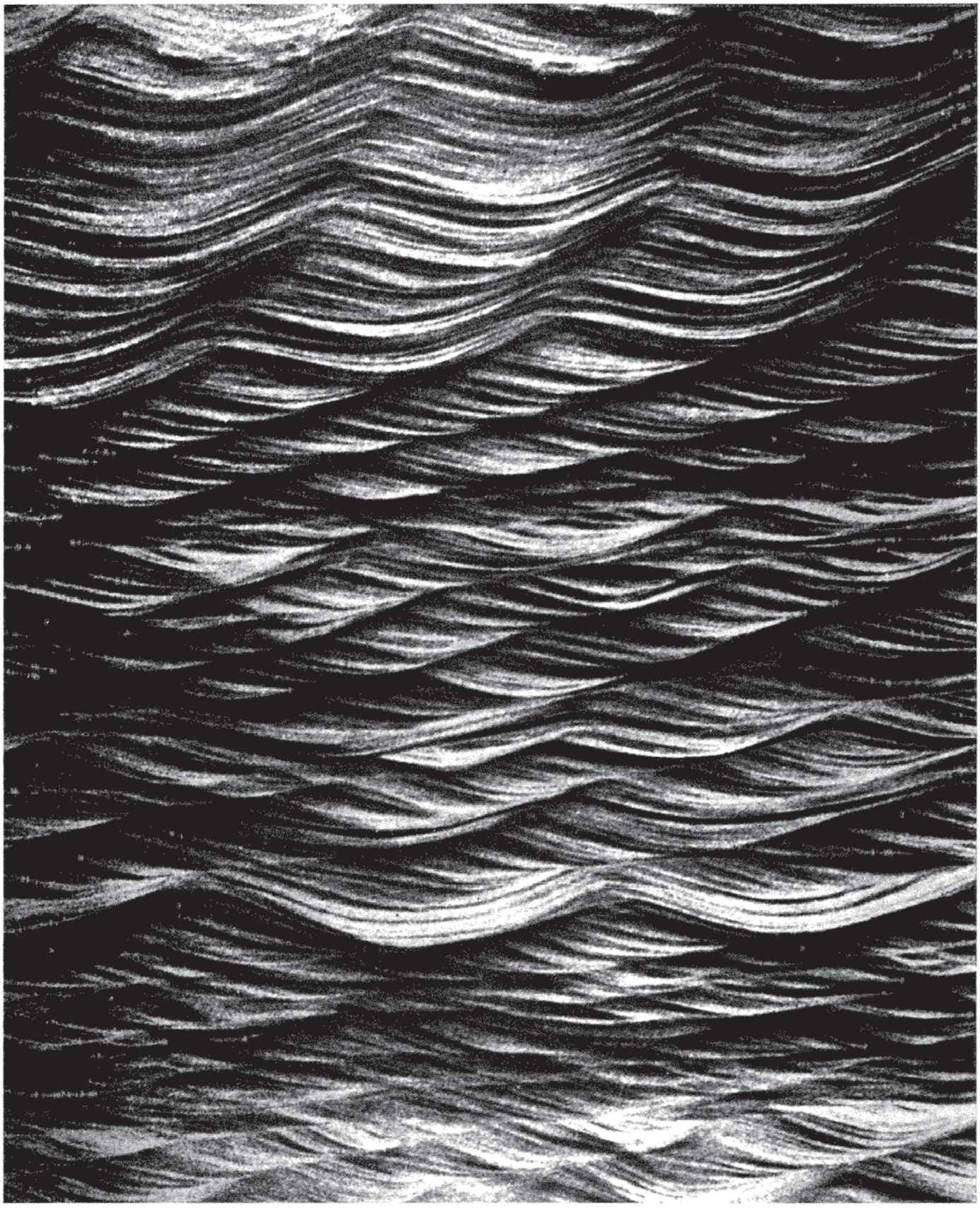

Close-up of aggrading ripples (climbing ripple drift) from the Colorado River, Arizona. These bedforms are indicative of a rapid unidirectional flow with excess sediment supply. (Photo courtesy of Paul E. Potter.)

4

Sedimentary Structures

Now that we have briefly discussed the physics of moving particles, we can examine how physical principles are manifested in the properties of the rock itself, particularly in the macroscopic **sedimentary structures**. Sedimentary structures or combinations of structures are often the best clue to the sedimentary environment because particular types of structures result from particular depositional processes.

PHYSICAL STRUCTURES

Physical (inorganic) structures are sedimentary features formed by physical processes without the influence of organisms. The most important of these are primary sedimentary structures, which are mechanical structures formed during deposition of the sediments. They do not include features formed during diagenesis.

Plane Bedding

The simplest sedimentary structure is plane bedding. Simple horizontal beds form in practically all sedimentary environments and under a variety of conditions, so further descriptive detail is needed to interpret them. Bedding is so common in sedimentary rocks that its origin is often overlooked because it is assumed to be inevitable. Three basic mechanisms can form plane bedding: sedimentation from suspension, horizontal accretion from a moving bedload due to a change in the competence of a flow, and encroachment into the lee of an obstacle. Plane beds often represent rapid deposition, usually by a single hydrodynamic event. Most deposited beds have been reworked, however, so *preservation potential* is also important. For example, submarine landslide deposits are buried rapidly, so they have a high preservation probability, but beach deposits are almost always reworked after they are deposited.

Finer-scale plane bedding (less than 1 cm thick) is usually called **lamination**. A number of mechanisms can form laminae. The classic example is the alternation of light and dark layers, such as glacial varves (Fig. 4.1). Alternation of mineral composition also occurs, as is seen in heavy mineral lags among the normal quartz sands on some beaches. Lamination can also result from the alternation of grain sizes caused by changes in the strength of the current during deposition. In some cases, apparent lamination is not a primary feature at all but is a secondary color banding due to diagenetic effects.

Lamination in muds is usually the result of slow, steady deposition. An absence of lamination in mudstones is probably due either to flocculation (clumping of clays before they settle) or to secondary **bioturbation** (disturbance by organisms). Usually, laminated sands have been deposited rapidly, often by a single hydrodynamic event such as the swash-

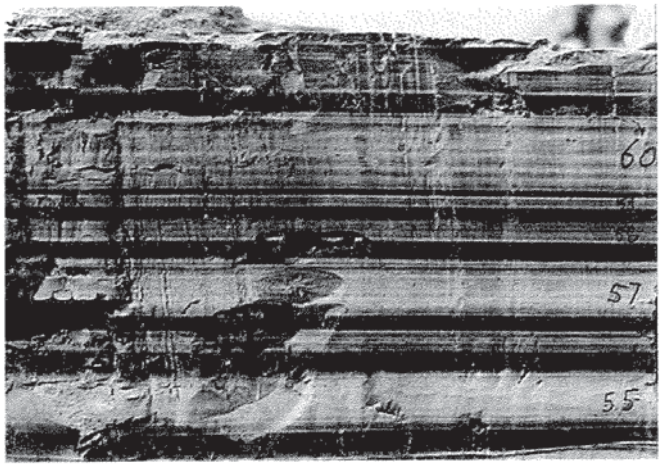

Figure 4.1

Seven years of Pleistocene varves near Seattle, Washington. Total thickness shown is about 12 cm. (Photo courtesy of J. Hoover Mackin.)

backwash of surf; traction by steady flow; the avalanching of sand down a dune face; or the migration of ripples, which leaves a heavy mineral lag. Truly massive deposits that show no bedding are anomalous. Such deposits often show cryptic bedding when studied by X-ray techniques or when stained (Fig. 4.2). The lack of plane bedding is usually a result of bioturbation, deposition from highly concentrated sediment dispersions, or rapid deposition from suspension.

Bedforms Generated by Unidirectional Currents

As soon as flow attains a force sufficient to erode particles from the bed, sediments are transported in a set of structures on the surface of the bed called

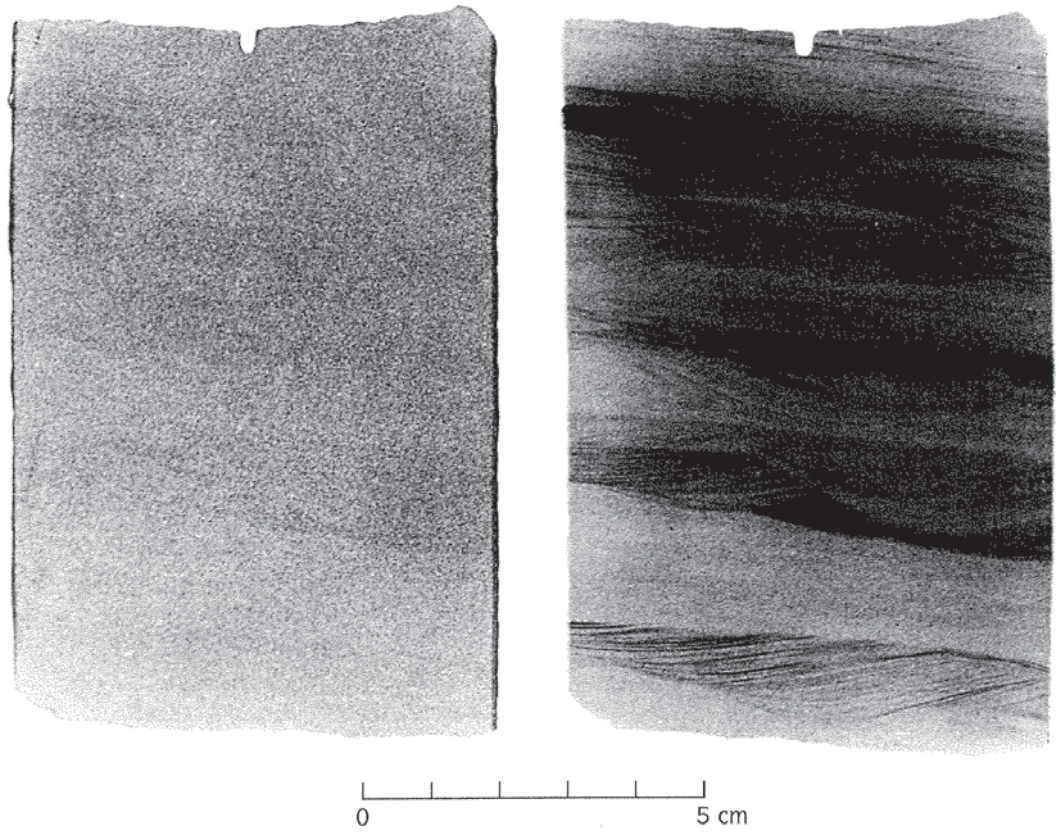

Figure 4.2

A polished slice of core (*left*) and a positive print of an X-radiograph (*right*) of Berea Sandstone (Mississippian), Illinois. Only vague banding is visible on the polished slab, but X-radiation reveals an apparent dip of 10°, scour and fill, and cross bedding. (From Hamblin, 1965.)

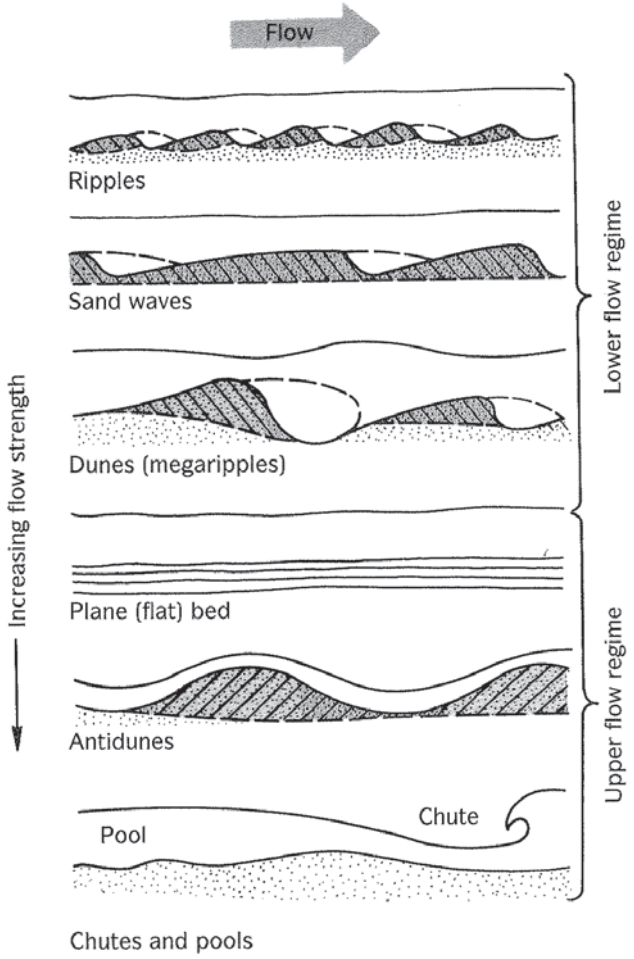

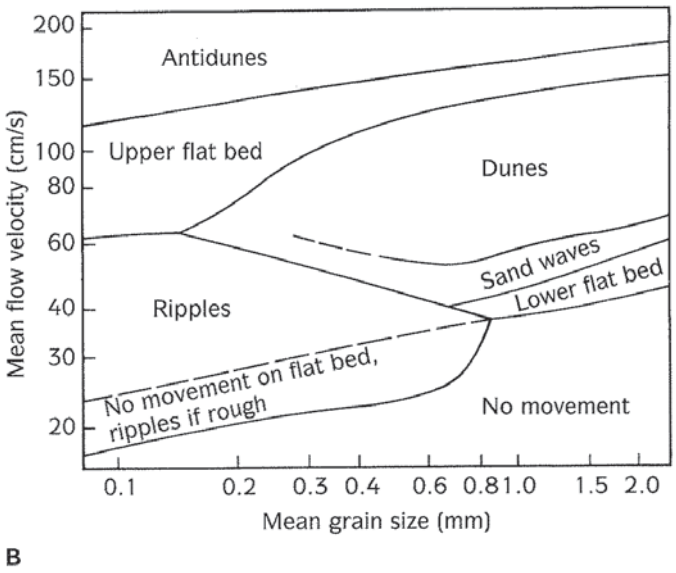

Figure 4.3

(A) Sequence of bedforms produced through increasing flow strength conditions. (From Blatt et al., 1980, *Origin of Sedimentary Rocks*, 2nd ed., p. 137; by permission of Prentice-Hall, Inc., Englewood Cliffs, N.J.) (B) Changes in bedforms resulting from different flow velocities (vertical axis) and grain sizes (horizontal axis). (From Lewis, 1984.)

bedforms. If these bedforms are later buried and preserved, they can form sedimentary structures. Flume studies have shown that there is a predictable sequence of bedforms that depends on velocity, grain size, and depth of flow (Fig. 4.3A). In sand that is finer than 0.7 mm (coarse sand or finer), the first features to form are *ripples*. Typically, their spacing is 10 to 20 mm or less, and their height is less than a few centimeters. As the flow velocity increases, the ripples enlarge until they form sand waves and finally dunes, which have spacings from 0.5 to 10 m or more and heights of tens of centimeters to a meter or more (Fig. 4.3B).

In deeper currents, greater flow velocity is required to produce the larger bedforms. Changes in water temperature or clay content alter the viscosity of the flow and thus affect the settling velocity. These factors alter the bedforms regardless of the other variables. Ripples, sand waves, and dunes all form in much the same manner. Small irregularities on the surface of the streambed cause a slight turbulence as the flow is diverted up and around them. Eventually, the flow over an obstacle no longer hugs the bottom but separates from it at the **point of flow separation** (Fig. 4.4), which is at the crest of the ripple or dune. The flow meets the bottom again at the **point of flow reattachment.** Beneath this zone of laminar flow is the zone of turbulence and backflow on the lee side of the ripple. This is the **zone of reverse circulation.** Sediment migrating up the ripple or dune avalanches down into this zone and is deposited by the weaker currents. This process generates the inclined foreset beds that produce cross-bedding. Because the ripple or dune is eroded on the upstream side and accreted on the downstream side, these bedforms migrate downstream. Meanwhile, most of the fine-grained suspended load of silt and clay is carried downstream, resulting in segregation of grain sizes.

The shape of the ripples depends primarily on a balance between the bedload and the material that is settling from suspension. If there is little suspended load, the ripples are steep, with a sharp angle between the foreset and bottomset beds. If there is a

large suspended load, the lee slope builds steadily, forming curved cross-strata and a tangential contact between foreset and bottomset beds. Ripples and dunes are dynamic features that change constantly. The downstream end of the zone of backflow (the point of reattachment) fluctuates continuously, so only its approximate position can be identified. Beyond the point of reattachment, turbulent eddies scour downstream and form troughs with their long axes parallel to the flow. As the ripples or dunes migrate downstream, they fill the troughs in front of them. This natural association of troughs and ripples produces normal trough cross-stratification.

Dunes form by the same processes as ripples, only on a much larger scale (centimeters in the case of ripples, meters in the case of dunes). Whereas ripples are unaffected by changes in depth and are strongly affected by changes in grain size, dunes are more strongly affected by depth and less affected by grain size. Dune height is limited only by depth of flow, but ripples can reach only a certain maximum height. Ripples tend to migrate in one plane (except in the case of climbing ripple drift, discussed later). Dunes, on the other hand, often migrate up the backs of other dunes.

With increased flow velocity, dunes are destroyed, and the turbulent flow, which was out of phase with the bedforms, changes to a sheetlike flow, which is in phase with the bedforms. This point is also marked by Froude numbers greater than 1, indicating that the flow has become rapid, shooting, or supercritical. Intense sediment transport takes place along **plane beds** (see Fig. 4.3A), which are produced by deposition of planar laminated sands. At even higher velocities, plane beds are replaced by **antidunes**, which produce low, undulating bedforms that can reach 5 m in spacing. Their fundamental feature is that their crests are *in phase* with the

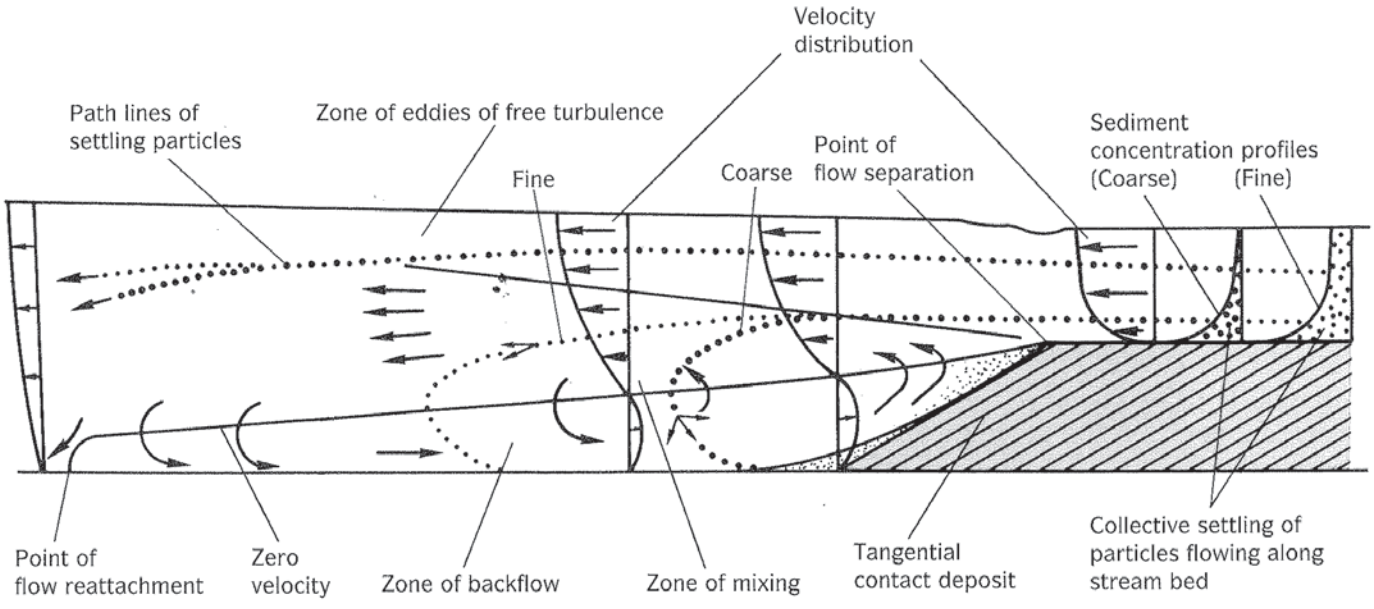

A

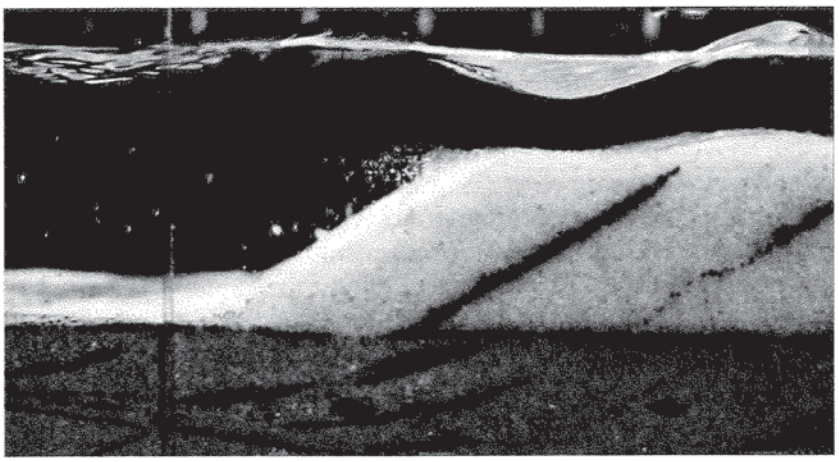

B

Figure 4.4

(A) Flow pattern and sediment movement over migrating ripples or dunes. Velocity profiles are shown by the vertical lines. (After Jopling, 1967, *Geology* 75:298, Fig. 19; copyright © 1967, by permission of the University of Chicago Press.) (B) In a laboratory flume, the trajectories of sand grains on the lee side of a ripple (migrating from right to left) can be seen. Layers of dark sand are also included to show the development of cross-bedding. (From Siever, 1988, *Sand*, p. 65; photo courtesy of A. V. Jopling.)

surface waves, so they migrate by accretion on the upstream side. In ancient deposits, antidunes are characterized by faint, poorly defined laminae. Antidunes generally show low dip angles (less than 10°) and are associated with other indicators of a high flow velocity. Because they migrate upstream, antidunes should leave evidence of a flow contrary to the flow direction shown by other current-direction indicators (see Box 4.1). It seems that antidunes are rare in the rock record, probably because they are reworked where the current slows before final burial. Finally, at the highest flow velocities, the antidunes wash out and are replaced by chutes and pools (see Fig. 4.3A).

The three-dimensional geometry of cross-stratification is a useful indicator of flow and sediment load. Starting with stationary current ripples (Fig. 4.5A), simple trough cross-stratification develops from migrating ripples and dunes (Fig. 4.5B). Tabular cross-stratification (Fig. 4.5D), on the other hand,

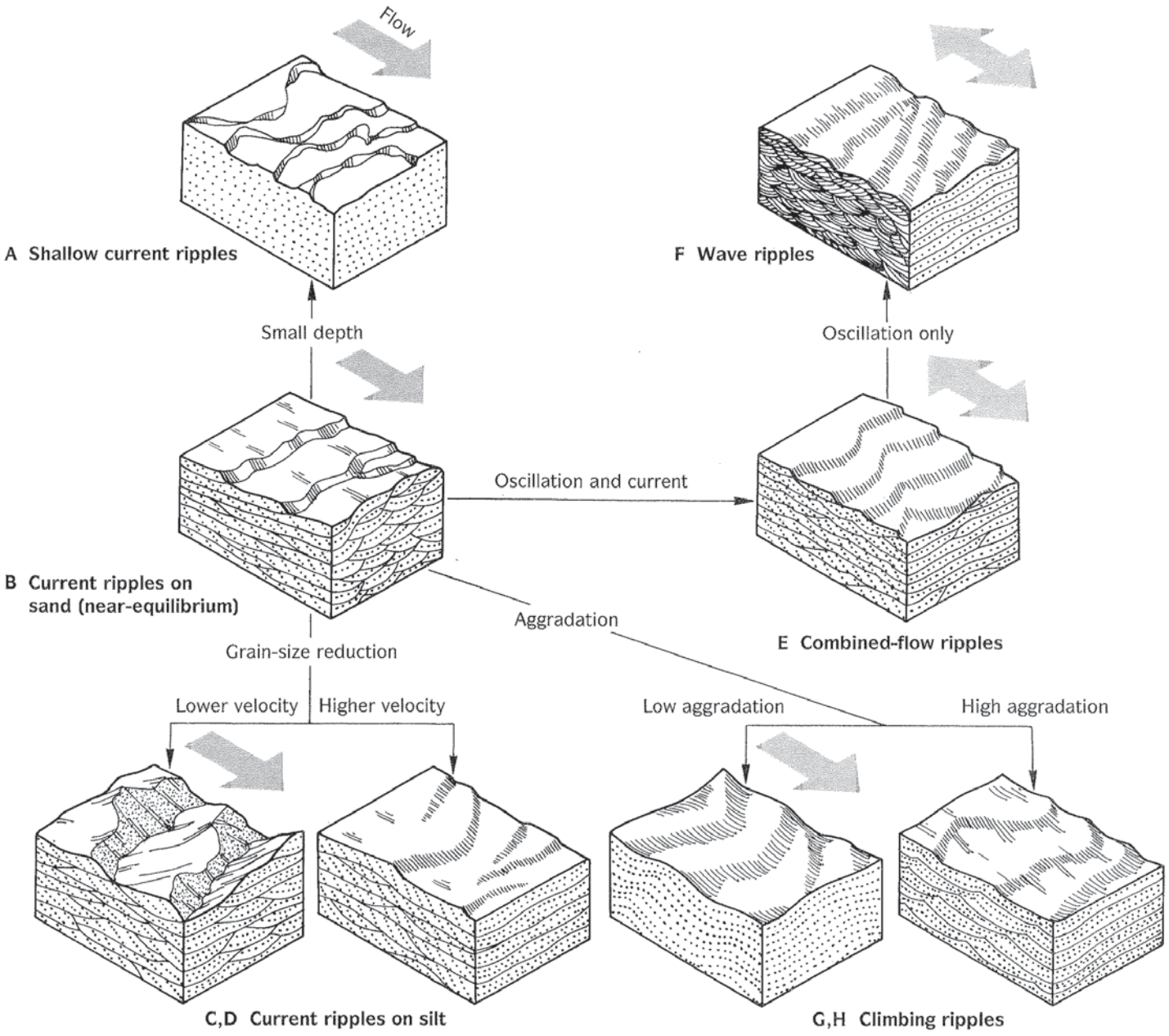

Figure 4.5

Variations in ripple forms and stratification caused by changes in velocity, grain size, depth, rate of sediment supply, and flow direction. (From Harms, 1979, *Ann. Rev. Earth Planet. Sci.* 7:236, Fig. 8; copyright © 1979 Annual Reviews, Inc.)

Box 4.1 Paleocurrent Analysis

Sedimentary structures can be used to interpret depositional environments and ancient hydraulics in many ways. One of the most valuable pieces of data is the flow direction indicated by unidirectional or bidirectional currents. For example, the flow direction and source of ancient river systems can often be determined from ancient cross-bedding orientations; the downslope direction of turbidity current can be determined from the orientation of flute marks and other directional sole marks. Paleocurrents may be crucial to testing certain hypotheses. For example, if the flow is unidirectional, flowing away from ancient source areas, and perpendicular to the ancient shoreline, it is probably fluvial or deltaic in origin. If the cross-beds are bidirectional, perpendicular to the shoreline, and 180° apart, they were probably caused by onshore-offshore tidal currents or waves. Unidirectional marine paleocurrents oriented parallel to the shoreline might be the result of longshore currents. Such information could be used to determine whether a cross-bedded sandstone in the marine-nonmarine transition is fluvial-deltaic, tidal, or longshore current in origin.

A number of paleocurrent features can be measured, including tabular and trough cross-bedding, the trends of channel axes, the alignment or imbrication of fossils or clasts, grain alignment in sandstones, sole marks (especially flute casts, drag marks, and groove casts), current and oscillation ripples, and even overturned soft-sediment folds (they indicate downslope). If these structures are well exposed in flat-lying strata, their trend or azimuth can be measured directly with a Brunton compass. In deformed strata, however, this trend must be corrected for the dip of the bedding. This is done using a stereonet.

First, the dipping plane of the bedding is represented as a great circle on a piece of tracing paper (Fig. 4.1.1). Then the paper is rotated to place the strike of the great circle along the north-south axis. The angle, or **rake,** between the current structure and the strike line (as measured in the field) is then plotted along the great circle (Fig. 4.1.2A). This gives an apparent azimuth of the paleocurrent direction (260° in this example). Finally, the bedding plane is rotated back to horizontal (Fig. 4.1.2B). During this rota-

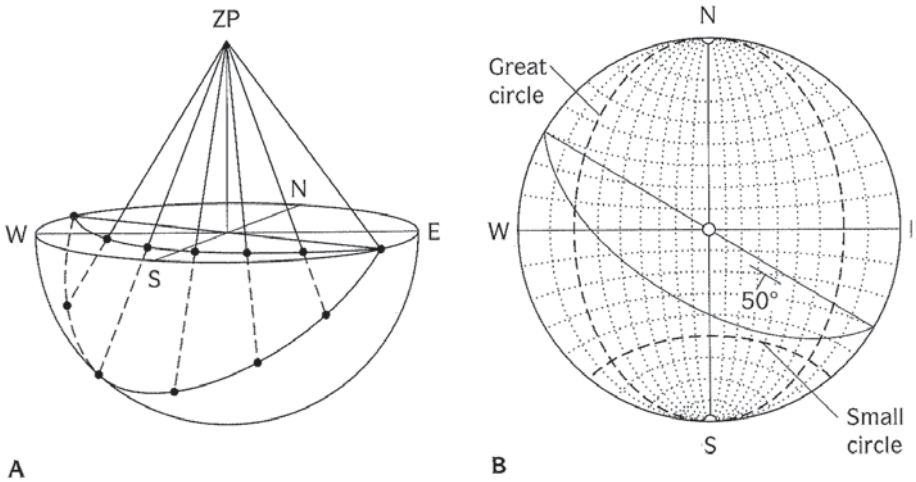

Figure 4.1.1

The stereonet is used to visualize three dimensions on a two-dimensional plot. (A) Projections of a plane with a dip of 50° and a dip direction of 210° (strike N60°W, dip 50°SW.) ZP, zenith point. (B) Stereographic projection of the plane shown in (A.) Also shown are projections of great circles (intersection of a sphere with any plane passing through the center of the sphere) and small circles (intersection of a sphere with any plane not passing through the center of the sphere.) (From R. C. Lindholm, 1987, *A Practical Approach to Sedimentology,* Fig. 2.1, p. 44; by permission of Allen and Unwin, London.)

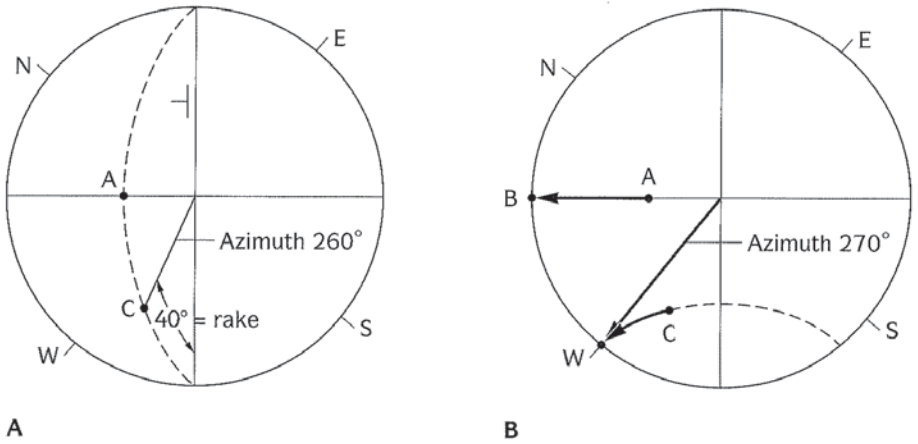

Figure 4.1.2

The correction of a linear structure for tectonic tilt using the stereonet. (A) Plot the plane of bedding as a great circle and the linear structure as a line. In this example, the bedding has a dip of 50° and a dip direction of 320° (strike N50°E, dip 50°W.) The rake of the linear structure is 40°; the azimuth of a vertical plane, which passes through the linear structure, is 260°. (B) Restore the bedding to horizontal (point A to point B.) Move the intersection point of the linear structure with the great circle projection of the bedding point (point C) along the nearest small circle (dotted line) to the edge of the stereonet. Read the azimuth of the linear structure. In this example, it is 270° (due west.) (From R. C Lindholm, 1987, *A Practical Approach to Sedimentology,* Fig. 2.2, p. 44; by permission of Allen and Unwin, London.)

tion, the intersection between the paleocurrent and the plane of the bedding will also rotate along one of the small circles to the edge of the stereonet (horizontal). This gives the true trend of this current in the horizontal plane. (For bedding dips of less than 25°, the difference between corrected and uncorrected paleocurrents is so slight that it is not necessary to correct at all).

In other cases, we have only side views of the structure in three dimensions and cannot see the trend of the flow in outcrop clearly. For example, a rock may protrude and give two different views of the cross-bedding (as exposed by random joint faces), but there are no faces that are exactly perpendicular to the flow direction to allow measurement of the true trend. In these instances, we can measure the apparent dip of the cross-bedding on each of two faces in a single cross-bed set. We also measure the strike and dip of each of the two rock faces. On the stereonet, these are shown as great circles, and the two apparent dips occur as points on each great circle. Rotating the stereonet so that these two points align along a common great circle produces the great circle of the plane of the cross-bedding dune or ripple face. The dip direction of this plane is the true current direction.

If there are more than two or three paleocurrents, a summary of the vectors is needed. The most common of these is known as a **rose diagram** (Fig. 4.1.3). In these plots, the compass is divided into convenient sectors (like the segments of an orange), typically of 20° to 30° of arc. All the corrected paleocurrent vectors that fall within a given sector are then summarized as "pie wedges," with the length of the pie wedge indicating the total number of vectors in that segment. The rose diagram shows the degree of scatter within unidirectional currents and often reveals that there are bimodal or polymodal vectors in the data set, indicating highly variable or multidirectional currents. Through visual inspection and comparison with other data, the significance of each mode should be apparent.

Although the rose diagram gives a good visual representation of the vector trend and the scatter of the data, a more rigorous statistical analysis is needed (especially if we want to compare rose diagrams from two or more places).

(*continued*)

(continued from page 49)

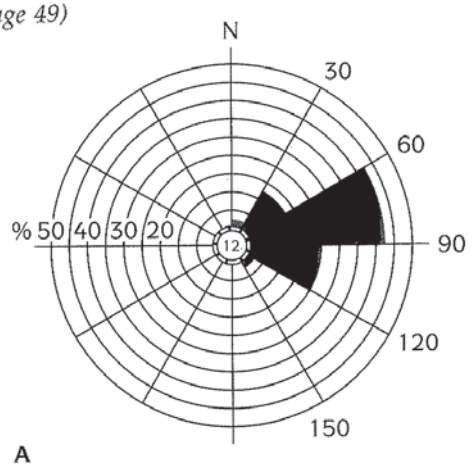

A

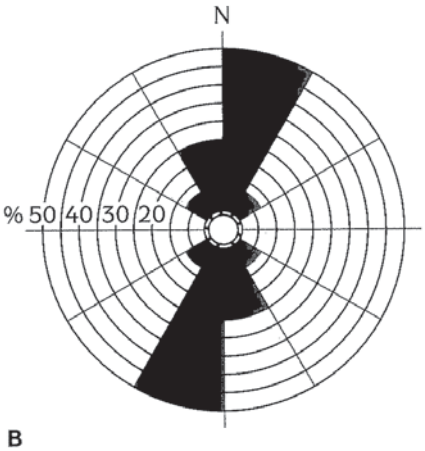

B

Class (degrees)	Number of observations	%
0–29	1	8
30–59	2	17
60–89	5	42
90–119	3	25
120–149	1	8
	12	100

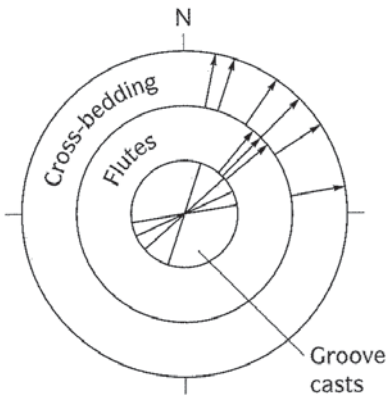

C

Figure 4.1.3

Rose diagrams. The diagrams may show (A) direction of movement data (12 cross-bed dip azimuths in degrees); or (B) line of movement data (compass bearing of 8 groove casts in degrees); or (C) data from several different structures (compass bearing of 4 groove casts, 3 flute casts, and 6 cross-bed azimuths.) (From R. C. Lindholm, 1987, *A Practical Approach to Sedimentology,* Fig. 2.4, p. 46; by permission of Allen and Unwin, London.)

Two common methods (graphical and trigonometric) are shown in Fig. 4.1.4. Once the vector mean is known, we also need to know the scatter of the vectors, or vector dispersion, known as the **consistency ratio** (analogous to the standard deviation in univariate statistics). These ratios allow a more rigorous comparison, such as determining whether two vector distributions are statistically the same or clearly come from different directions.

is produced by migrating sand waves. Horizontal stratification can be produced by plane-bed conditions at high flow velocities. Often, the migration of a ripple is interrupted; the ripple is eroded back and then buried by a new advancing bedform. Such an interruption produces a tiny erosional surface between cross-strata, known as a **reactivation surface** (Fig. 4.6).

Figure 4.5 shows the natural sequence of ripple features resulting from changes in flow conditions, grain size, and sediment supply. As flow increases, incipient ripples develop into full-scale trough cross-

Azimuth		sin x	cos x
1	27°	+0.4540	+0.8910
2	172°	+0.1392	−0.9903
3	68°	+0.9272	+0.3746
4	112°	+0.9272	−0.3746
5	50°	+0.7660	+0.6428
6	123°	+0.8387	−0.5446
7	100°	+0.9480	−0.1736
8	137°	+0.6820	−0.7314
9	160°	+0.3420	−0.9397
10	111°	+0.9336	−0.3584
11	118°	+0.8829	−0.4695
12	146°	+0.5592	−0.8290
13	80°	+0.9848	+0.1736
14	96°	+0.9945	−0.1045
15	77°	+0.9748	+0.2250
Σn		+11.3541	−3.2085

$$\tan x = \frac{\Sigma n \sin x}{\Sigma n \cos x} = \frac{11.3541}{-3.2085} = -3.539$$

arctan $-3.539 = -74°$ or $106°$ = vector mean

$$R = \sqrt{[(\Sigma n \sin x)^2 + (\Sigma n \cos x)^2]}$$

$$R = \sqrt{(128.91 + 10.29)} = 11.8$$

$$L = \frac{R}{n} \times 100 = \frac{11.8}{15} \times 100 = 79 = \text{vector magnitude}$$

A

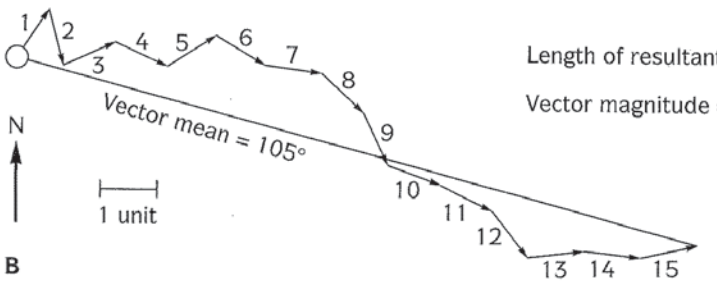

B

Length of resultant vector = 12 units

Vector magnitude = $\frac{12}{15} = 80\%$

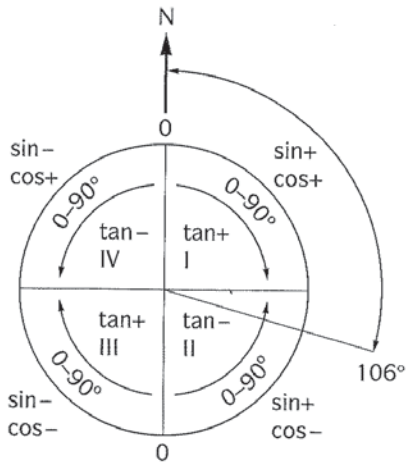

Figure 4.1.4

Methods for calculating vector mean and vector magnitude. (A) Trigonometric method. The tangent of the mean vector is calculated by dividing the sum of the sines by the sum of the cosines. The vector mean is the arctan of this value. The *signs* of the trigonometric functions must be recorded accurately. In this example, the negative tangent (positive sine and negative cosine) lies in the second quadrant, and the resultant azimuth (−74°) is plotted counterclockwise from zero at the bottom of the circle. According to standard geologic usage, this equals 106° (measured clockwise from zero, or due north), or S74°E in the quadrant scheme of some compasses. The vector magnitude in percent (L) is determined by dividing R (11.8) by the number of measurements (15) multiplied by 100. (B) Graphical method. Each measured azimuth is plotted as a unit vector. One unit of length can be 1 cm, 1 inch, or whatever is convenient. In this illustration, the unit vectors are labeled 1 to 15 (azimuths given in A above.) The resultant vector, or the line that connects the origin to the end of the last unit vector, is the vector mean. The vector magnitude is obtained by dividing the length of the resultant vector (12 units) by the total length of the unit vectors (15 units) and multiplying by 100. (From R. C Lindholm, 1987, *A Practical Approach to Sedimentology*, Fig. 2.5, p. 48; by permission of Allen and Unwin, London.)

beds at equilibrium. If the grain size then decreases, the shape of the current ripples changes, depending on flow velocity (Fig. 4.5C, D). If the current becomes less unidirectional, sinuous combined-flow ripples result (Fig. 4.5E). A fully oscillatory current (such as in waves) produces straight, symmetrical ripple marks with a distinctive lenticular cross section (Fig. 4.5F; see also Fig. 10.8). If the sediment supply increases, then the ripples build upward, or **aggrade.** Low aggradation produces **climbing ripples** (Fig. 4.5G; see also p. 42). High aggradation produces sinuous ripples that are in phase (Fig. 4.5H).

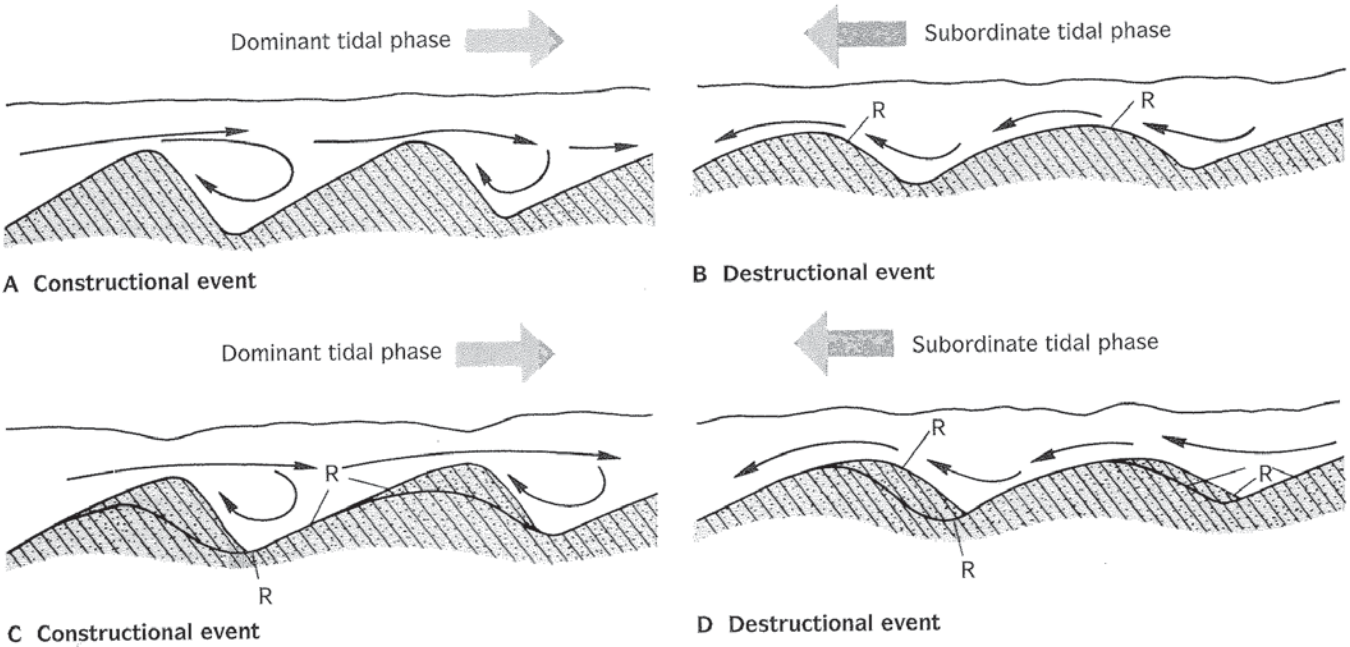

Figure 4.6

Sequence of events that form reactivation structures. The dominant tidal phase builds cross-beds (A), which are eroded back during tidal retreat (B.) The return of the constructional tide buries this erosional reactivation surface, R, with new cross-beds (C), and the process repeats (D). (After Klein, 1970.)

Bedforms Generated by Multidirectional Flow

Although they are formed in a different manner, wave ripples on beaches are similar to current ripples. A rotating eddy precedes a wave as it moves onshore, precipitating the sand load into troughs and ripples. As the wave crest passes, the eddy rises with the crest and disperses into the backwash. The coarser grain sizes are left on the beach, and the finer sand is washed offshore, so beach sands are very well sorted. Wave ripples are not easy to distinguish from current ripples, but there are some differences. Wave ripples are usually symmetrical (or only slightly asymmetrical) with peaked crests and rounded troughs. If they are asymmetrical at all, they indicate a current direction toward the shore. Their cross-laminae also dip shoreward.

Other waveforms are confined to tidal regions. Unlike on the beach, fine sediment in the tidal zone is moved onshore because incoming tides flow in slowly, allowing the sediment to settle. Retreating tides move out too slowly to scour away much of this deposition. As a result, tidal ripples are generally unidirectional, with weak backflow structures. Cross-beds are oriented in two directions, often with reactivation surfaces caused by the reversal of current direction during a tidal cycle. This is known as **herringbone cross-bedding** (Fig. 4.7). The bidirectionality of tidal outflow currents often superimposes a weaker ripple system on the dominant sinuous ripples produced by rising tides. These two systems produce **interference ripples,** or "tadpole nests" (Fig. 4.8). The most distinctive features of tidal regions are caused by the mixing of sand- and mud-sized fractions from the asymmetrical currents. Small lenses of sand in muddy beds, called **lenticular bedding** (Fig. 4.9A, B), occur when sand is trapped in troughs in the mud as sand waves migrate across a muddy substrate. If mixing produces minor mud layers in a sandy substrate, the pattern is called **flaser bedding** (Fig. 4.9A, C). An equal mixture of sand and mud (Fig. 4.9A) characterizes **wavy bedding.**

Wind-transported sand behaves differently from water-transported sand, although wind-generated ripples look superficially like water-generated ripples. Sand particles in wind move mostly by saltation (jumping and bouncing) and to a lesser extent by surface creep. Particles that are too large to move by saltation and creep accumulate as a lag, forming a

Figure 4.7

Herringbone cross-stratification from alternating tidal currents, Cambrian Cadiz Formation, Marble Mountains, California. (Photo by D. R. Prothero.)

A

B

Figure 4.8

(A) Interference pattern formed in symmetrical ripples from two coexisting wave sets in a modern tidal flat. (Photo courtesy of J. D. Collinson.) (B) Ancient interference ripples from the Cambrian Cadiz Formation, Marble Mountains, California. (Photo by D. R. Prothero.)

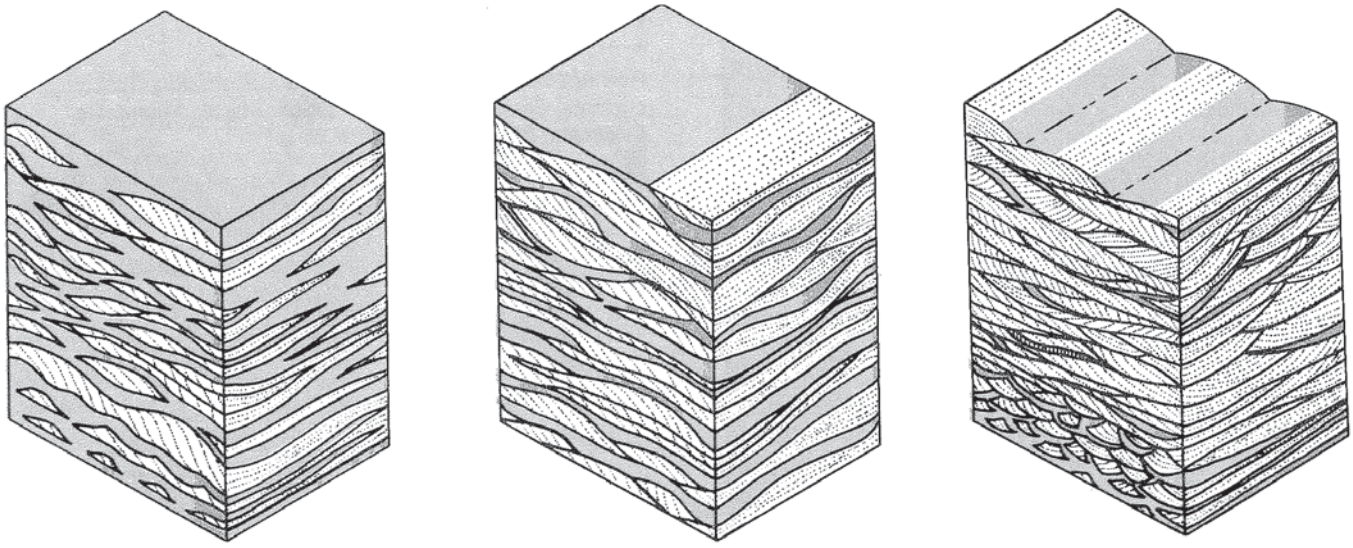

A

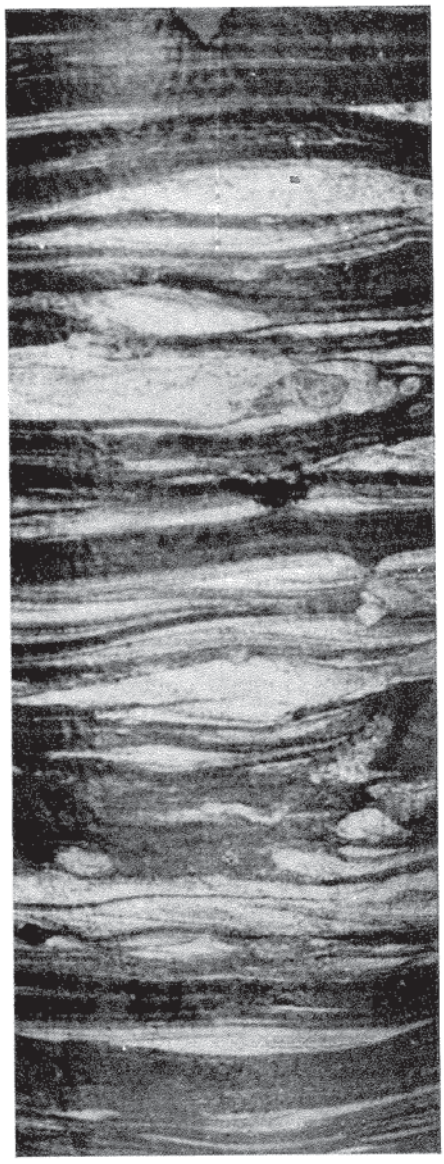

B

C

Figure 4.9

(A) Diagrams showing lenticular, wavy, and flaser bedding. (B) Core showing lenticular bedding of sand lenses within a predominately muddy sequence from the Mississippian Tar Springs Sandstone, Illinois. (C) Core showing flaser beds of mud stringers within a sandy sequence from the Pennsylvanian Carbondale Formation, Illinois. (Photos B and C from F. J. Pettijohn and P. E. Potter, 1964, *Atlas and Glossary of Primary Sedimentary Structures*, plates 18B and 17B; reprinted by permission of Springer-Verlag, New York.)

desert pavement in areas of wind deflation. Because saltation is more effective than scouring in moving sand, erosion is heaviest on the exposed upwind side of a sand dune, where the impact of windblown particles is greatest. Deposition occurs on the protected lee side; because there is no zone of backflow, the lee sides do not scour. This is the opposite of water ripples, which erode on the lee side.

Wind ripples migrate by eroding on their upwind side and building on their downwind side until they reach an equilibrium size for the wind strength and sand supply. They are usually composed of sand that is coarser than the substrate over which they migrate, and their crests are made of coarser particles than their troughs. Water ripples show the opposite condition in both these features. Wind ripples form by the winnowing of their crests, which leaves the coarser material behind, whereas water ripples accumulate coarser sediments in the troughs where the zone of backflow results in weaker currents and reduced competence. Another major difference is that wind ripples are not limited by the shallow flow depths that restrict water ripples, so eolian dunes can be enormous (meters to tens of meters in height). Indeed, gigantic cross-strata are virtually always found only in eolian environments (see examples in Chapter 8).

Bedding Plane Structures

The sedimentary structures just discussed are formed during the deposition of the bed and are generally three-dimensional. Another class of sedimentary structures forms on the interface between beds, usually on the exposed surface of a recently deposited bed before it is finally buried. Such structures can be extremely useful because they indicate current directions and postdepositional deformation of the sediment.

Sole marks, found on the bottom surfaces of beds, are usually casts or molds of depressions that were formed in the underlying beds by currents. The filling, or sole mark, tends to have a higher preservation potential because it is buried immediately as the depression is filled. The most common form of sole mark is a **flute cast** (Fig. 4.10), which is shaped like an elongated teardrop that tapers upcurrent. It is formed by a slight irregularity on a mud substrate that causes flow separation and a spiral eddy. The eddy spirals around a horizontal axis parallel to the flow and scours out the rounded, deep end of the flute cast. As the spiral eddy diminishes, the scouring becomes narrower until the point of the scour is reached. Another class of sole mark is the **tool mark**, which is an indentation of the cohesive mud bottom made by any object, or "tool" (Fig. 4.11). Tool marks include groove casts, brush marks, skip marks, chevron molds, prod marks, and bounce marks. These names describe the types of indentations that are left by the various objects (for example, twigs, branches, pebbles, shell fragments, and fish vertebrae) that produce them.

Subaerially exposed mud also produces sedimentary structures that can be useful in identifying sedimentary environments. The most familiar of these are mudcracks and raindrop impressions, which nearly always indicate drying of a subaerial mudflat (see p. 102). Because curling mudcracks always curl upward, they are also good indicators of the top side of a bed. In undeformed strata, such indicators may not be very important, but when beds

Figure 4.10

Flute casts from the Ordovician Normanskill Formation of New York. Flute casts are typically teardrop-shaped, with their tapered ends pointing downstream. The casts were produced when turbulent currents scoured the bottom and excavated tapered depressions. These flutes occur on the bottom surface of a turbidite bed, showing sole marks produced when the sediments forming this bed filled depressions in the layer that once underlaid it. The currents in this example flowed from lower right to upper left. (Photo courtesy of E. F. McBride.)

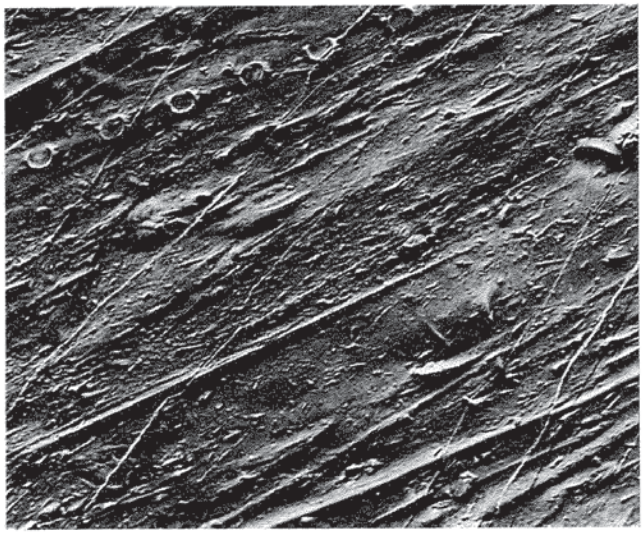

Figure 4.11

Tool marks from the base of the Carpathian flysch, Poland. The marks include circular skip casts from spool-shaped fish vertebrae, shallow brush marks, and deeper drag marks. (Photo courtesy of J. E. Sanders.)

have been structurally deformed, the top is not necessarily obvious. In such cases, it is crucial to find **geopetal** structures, which indicate the top of the bed. Cross-beds usually have truncated tops (because the next cross-bed set scours down into the previous one) and tangential contacts between foresets and bottomsets, so they can often be used to determine the top (see p. 136 and Fig. 8.24). Ripple crests are usually sharp, whereas ripple troughs are always rounded and scooped. Normally graded beds are clear indicators of the top because the coarsest material settles out first and is concentrated at the bottom (see Fig. 3.11B). Sole marks are found only on the base of the bed; the depressions that molded them are therefore on top of the underlying bed.

Soft-Sediment Deformation Structures

Sediment can be deposited so rapidly that the beds are unstable. In cases where denser material is deposited on top of less dense material, gravity tends to overturn it. If there is enough pore water, the whole mass can become liquefied like quicksand and be deformed. Large forces placed on the sediment before lithification can deform it while it is still soft. If a mass of sediment slumps (a common occurrence on slopes in the marine environment), the sed-

A

B

Figure 4.12

(A) Load casts from the Pennsylvanian Smithwick Formation, Burnett County, Texas. (Photo courtesy of E. F. McBride.) (B) Scaly or squamiform load casts (plus complex flute and groove casts) on the sole of an Ordovician turbidite that has been tilted vertically so that the bottom is exposed. (From Siever, 1988, *Sand*, p. 123; by permission of W. H. Freeman, New York.)

A B

Figure 4.13

(A) Ball and pillow structure seen from below; from the Oligocene Annot Sandstone, Peira-Cava, Maritime Alps, France. (B) Cross section of ball and pillow structure showing internal lamination conforming to the boundary of the pillow; from the Ordovician Cynthiana Group, Pendleton County, Kentucky. (Photos courtesy of P. E. Potter.)

iment can become internally deformed. All these processes produce distinctive deformation structures. The most common are **load structures,** irregular, bulbous features formed when a denser material has sunk into a less dense medium (Fig. 4.12). Sometimes, balls of sand load downward into underlying mud and then are pinched off, forming **pseudonodules,** or "ball and pillow" structures. These occasionally reach enormous dimensions (Fig. 4.13). Tonguelike protuberances of mud into overlying soft sediment are known as **flame structures** (Fig. 4.14). Finally, deformation of soft sediments leads to **convolute bedding** and other features that suggest intense structural deformation on a regional scale (Fig. 4.15). These features are formed shortly after deposition, however, and do not imply regional structural forces. Such features can easily fool the unwary geologist into postulating spurious structural events. The best way to distinguish convolute bedding from true structural deformation is to see whether it is widespread and penetrative or restricted to a single bed (see Fig. 10.12). Convolute lamination should also be associated with other more diagnostic soft-sediment deformation features.

Figure 4.14

Flame structures and graded bedding in upper Pleistocene lacustrine sediments, Fraser River Valley, British Columbia. Field of view is 35 cm wide. (Photo courtesy of A. Rodman.)

Figure 4.15

Convolute lamination in polished slabs of siltstone from the Martinsburg Formation (Ordovician), Pennsylvania. (From McBride, 1962.)

BIOGENIC SEDIMENTARY STRUCTURES

Sedimentary structures formed by organisms are known as **trace fossils**, ***Lebensspuren*** (German for "living traces"), or **ichnofossils** (Greek *ichnos*, "trace"). Besides their importance as paleontological objects, trace fossils are useful clues to depositional conditions. They are given taxonomic names as if they were valid Linnaean genera and species, but this is not really proper. Trace fossils are fossilized behavior, not body fossils. Few "ichnogenera" can be definitely associated with a known body fossil. It is likely that one type of trace was produced by several types of organisms or that one organism produced several types of traces. This taxonomy is analogous to giving a different species name to footprints produced by the same individual wearing different shoes. Nevertheless, the practice of giving Linnaean names to trace fossils is so well established that it persists for lack of a better system.

Certain characteristic trace fossils have been clearly associated with specific depth and bottom conditions (Fig. 4.16). These associations are known as **ichnofacies**. A working knowledge of the more common ichnogenera and ichnofacies is very important because these trace fossils are almost as diagnostic as index fossils for certain purposes. In the following paragraphs, we will review only the most commonly encountered ichnofossils and ichnofacies. For further details, consult Pemberton et al. (1992), Ekdale et al. (1984), Bromley (1990), and Frey and Pemberton (1985).

Skolithos Ichnofacies

Vertical tubelike burrows ("piperock") are commonly known as *Skolithos* and are believed to have been formed by tube-dwelling organisms that lived in rapidly moving water and shifting sands (Fig. 4.17A, B). Most of the tubes are 1–5 mm in diameter and can be as long as 30 cm. In some cases, they are densely clustered together and form thick layers of sandstone that resemble organ pipes (hence the name *piperock*). *Skolithos* piperock is particularly common in shallow marine Cambrian sandstones. The organism that made *Skolithos* is unknown, although some geologists have suggested phoronids (a burrowing wormlike lophophorate related to brachiopods) or tube worms. It is also possible that the trace-maker is extinct, since *Skolithos* is unknown after the Cretaceous.

Another common burrow in this ichnofacies is known as *Ophiomorpha* (Fig. 4.17A, C). These vertical cylindrical burrows are similar to *Skolithos*, except that they are slightly larger in diameter (0.5–3 cm)

and have a bumpy outer surface caused by fecal pellets that lined the burrow. Typically, they are also less densely clustered than *Skolithos* and may have short horizontal connecting burrows between the vertical tubes. In cross section, they appear as circular or oval structures, often with a dark ring of organic matter from the fecal pellet lining. Unlike *Skolithos*, however, we know what produces *Ophiomorpha* today (they are known back to the Permian.) The trace-maker is the burrowing ghost shrimp known as *Calianassa* (Fig. 4.17D).

A third common shallow marine ichnofossil is *Diplocraterion* (Fig. 4.17A, E, F). *Diplocraterion yoyo* tells a very specific story about the sea bottom. It is a burrow trace found between the arms of a vertical, U-shaped tube that presumably housed a burrowing, tubelike organism. When the openings were buried by sediment, the organism moved up in its burrow; when the upper part of the burrow was eroded away, the trace-maker dug in deeper. The sequence of U-shaped burrow traces thus responds like a yo-yo to the rise and fall of the sediment-water interface.

The characteristics of all of these burrows suggest a rapidly shifting substrate that requires organisms to dig deep vertical burrows that must be rebuilt often when waves wash them away. Most of the burrowing organisms appear to be filter feeders that use the sediment strictly for shelter, not as a source of food. In addition, sedimentological evidence also places this ichnofacies in shallow marine environments, and the known environmental preferences of living calianassid crustaceans further reinforces this interpretation. Thus, the *Skolithos* ichnofacies clearly indicates clean, well-sorted near-shore sands with high levels of wave and current energy.

Cruziana Ichnofacies

Horizontal U-shaped troughs with many intermediate, riblike feeding traces are known as *Cruziana* and occur in moderate- to low-energy sands and silts of the shallow shelf (Figs. 4.18, 4.19). *Cruziana* are often preserved as the cast of the trough-shaped burrow, forming a convex sole mark, rather than as the original concave burrow itself. Many *Cruziana* are believed to represent the feeding traces of trilobites (Fig. 4.19B), since they are long troughs that appear to bear the scratch marks of trilobite legs as they burrowed through the shallow sediment. Their occurrence in rocks of Cambrian through Permian age

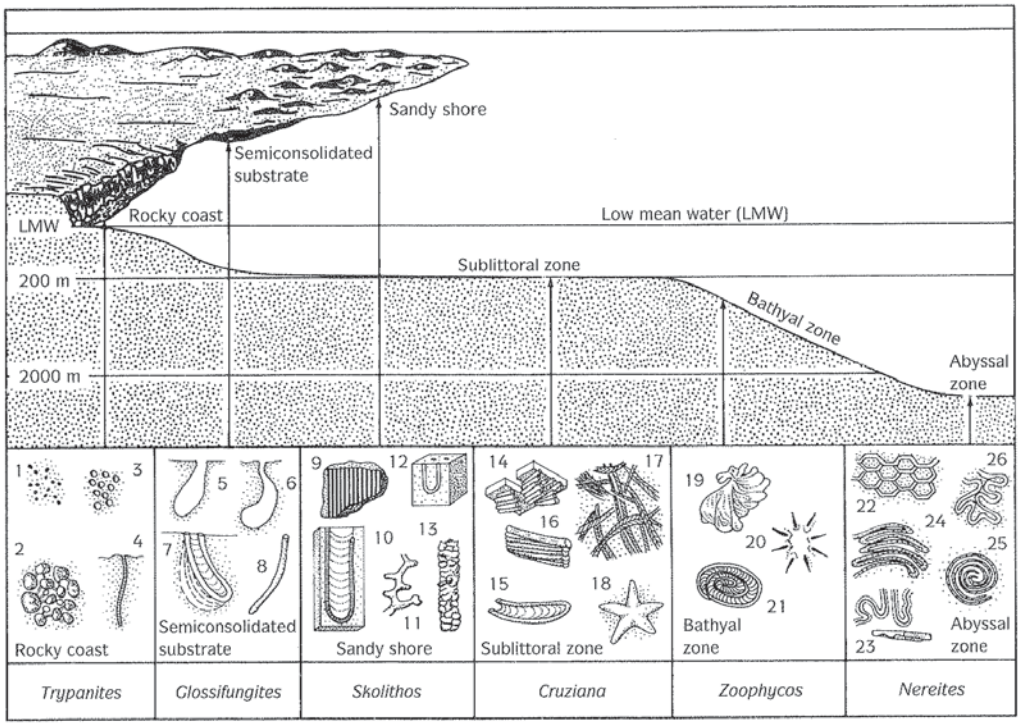

Figure 4.16

Summary diagram of the most common trace fossils and ichnofacies. Traces numbered as follows: 1 = *Caulostrepsis*; 2 = *Entobia*; 3 = unnamed echinoid borings; 4 = *Trypanites*; 5, 6 = *Gastrochaenolites* or related ichnogenera; 7 = *Diplocraterion*; 8 = *Psilonichnus*; 9 = *Skolithos*; 10 = *Diplocraterion*; 11 = *Thalassinoides*; 12 = *Arenicolites*; 13 = *Ophiomorpha*; 14 = *Phycodes*; 15 = *Rhizocorallium*; 16 = *Teichichnus*; 17 = *Crossopodia*; 18 = *Asteriacites*; 19 = *Zoophycos*; 20 = *Lorenzinia*; 21 = *Zoophycos;* 22 = *Paleodictyon*; 23 = *Taphrhelminthopsis*; 24 = *Helminthoida*; 25 = *Spirorhaphe*; 26 = *Cosmoraphe*. (From Frey and Pemberton, 1984, Trace fossil facies models, in R.G. Walker, ed., *Facies Models*, pp. 189–207; by permission of the Geological Association of Canada.)

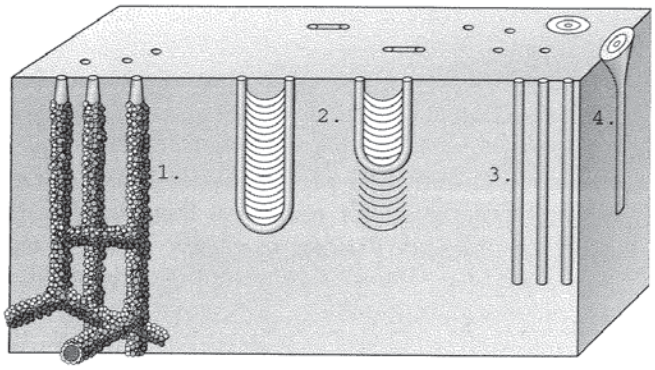

A

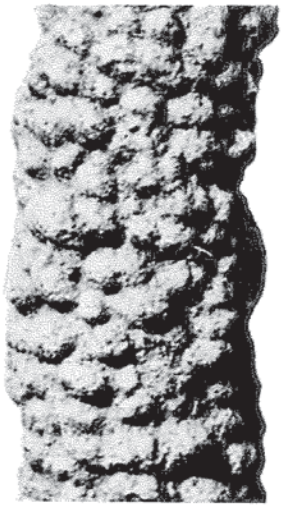

C

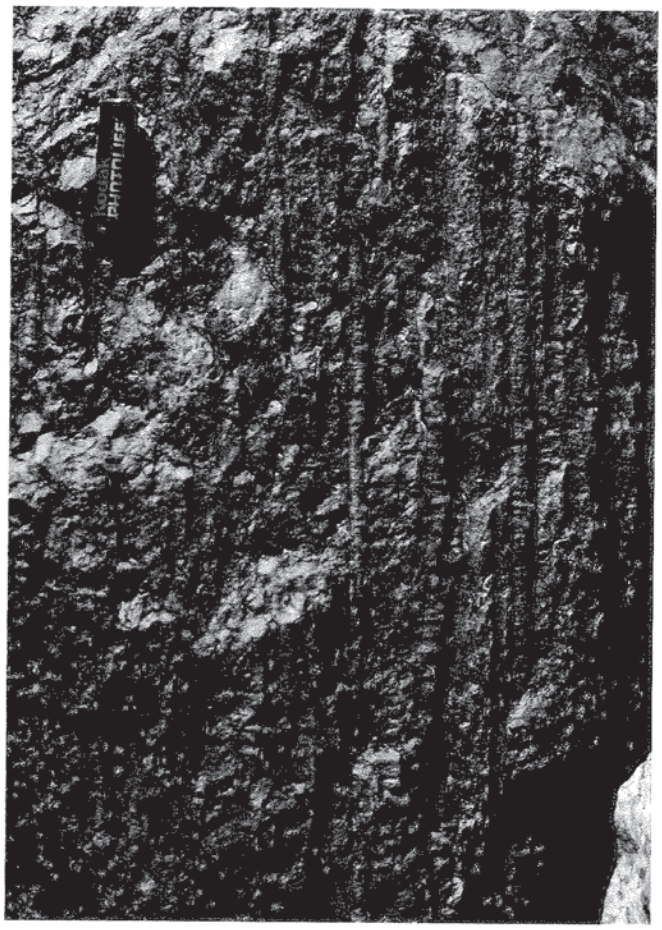

B

D

Figure 4.17

(A) Common trace fossils of the *Skolithos* ichnofacies. 1 = *Ophiomorpha;* 2 = *Diplocraterion;* 3 = *Skolithos;* 4 = *Monocraterion.* (Frey and Pemberton, 1984, Trace fossil facies models, in R. G. Walker, ed., *Facies Models*, pp. 189–207; by permission of the Geological Association of Canada.) (B) Side view of piperock showing numerous parallel *Skolithos* burrows, from the Cambrian Zabriskie Quartzite, Death Valley, California. (Photo courtesy of M. L. Droser.) (C) Side view of the pellet-lined burrow known as *Ophiomorpha*, from the Cretaceous Fox Hills Sandstone of the Denver Basin. (Photo courtesy of R. J. Weimer.) (D) The living ghost shrimp *Calianassa*, exposed in its burrow; it produces *Ophiomorpha* burrows today. (Photo courtesy of R. J. Weimer.) (E) Side view of *Diplocraterion* burrows from Lower Cambrian Prospect Mountain Quartzite, Cricket Mountains, Millard County, Utah. (Photo courtesy of A. A. Ekdale.) (F) Top views of *Diplocraterion* burrows (note the paired sets of holes) from the Lower Cambrian, Vik, Sweden. (Photo courtesy of A. A. Ekdale.)

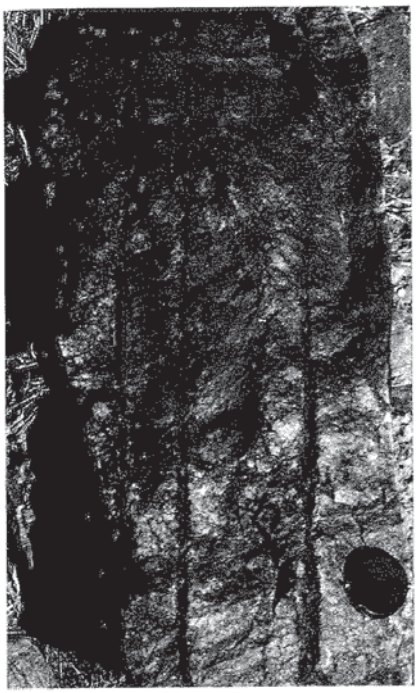

E

F

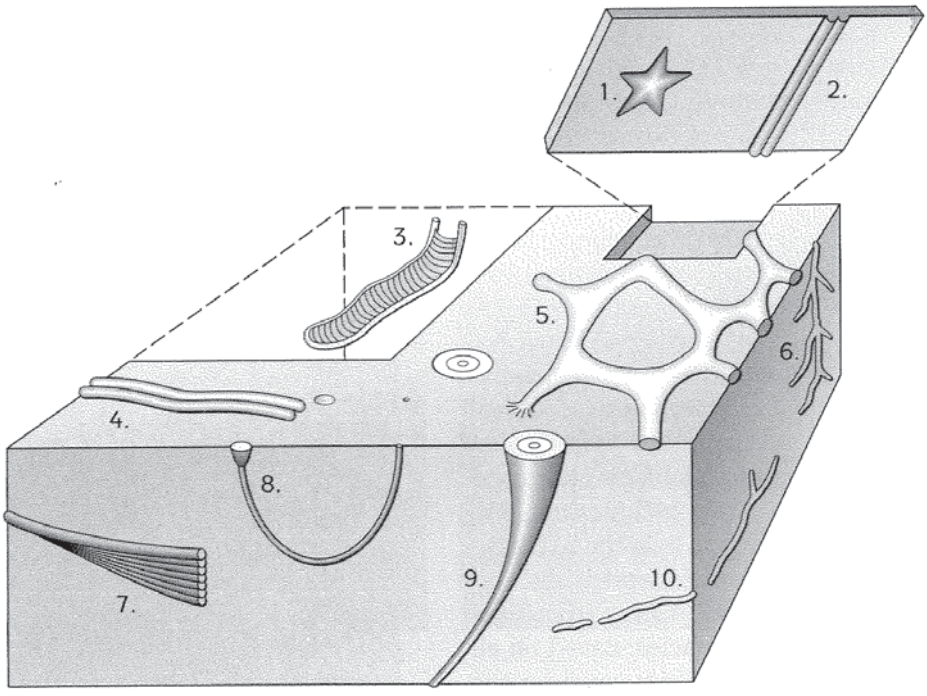

Figure 4.18

Common trace fossils of the *Cruziana* facies. 1 = *Asteriacites*; 2 = *Cruziana*; 3 = *Rhizocorallium*; 4 = *Aulichnites*; 5 = *Thalassinoides*; 6 = *Chondrites*; 7 = *Teichichnus*; 8 = *Arenicolites*; 9 = *Rossella*; 10 = *Planolites*. (From Frey and Pemberton, 1984, Trace fossil facies models, in R. G. Walker, ed., *Facies Models*, pp. 189–207; by permission of the Geological Association of Canada.)

A B

Figure 4.19

Cruziana traces appear as bilobate convex structures with parallel scratch marks from the legs of the burrowing trilobite as shown in (B.) (Photo courtesy of T .P. Crimes.)

(the same stratigraphic range as the trilobites) further reinforces this interpretation.

Another common trace fossil in this ichnofacies is *Thalassinoides* (Fig. 4.20). This is a general name for a complex three-dimensional network of cylindrical burrows that form an irregular web of crisscrossing tubes 1–7 cm in diameter. Apparently, this burrower was mining the shallow marine sands for their nutrients as well as seeking protection in its complex web of burrows. The organism or organisms that produced *Thalassinoides* are unknown, although some modern calianassid burrows resemble them.

In addition to these two typical ichnogenera, there are a number of other less common trace fossils that are characteristic of this ichnofacies. They include (see Fig. 4.18) the star-shaped *Asteriacites*, the U-shaped *Rhizocorallium* (like a horizontal *Diplocraterion*), the C-shaped *Arenicolites*, the conical *Rossella*, and the deeper horizontal burrows known as *Planolites*. Most are traces of organisms that used the substrate both as a shelter and to mine the sediment for food particles. *Cruziana* is also the most diverse of all ichnofossil communities, and it is commonly associated with finer sediments than are associated with the *Skolithos* ichnofacies. Based on all these lines of evidence, most specialists consider the *Cruziana* ichnofacies to be indicative of shallow marine waters below normal wave base but above storm wave base, typical of the middle and outer shelf. Indeed, the top surfaces of storm deposits are often overprinted by *Cruziana* ichnofacies activity that occurred on the fresh sea bottom right after a major storm.

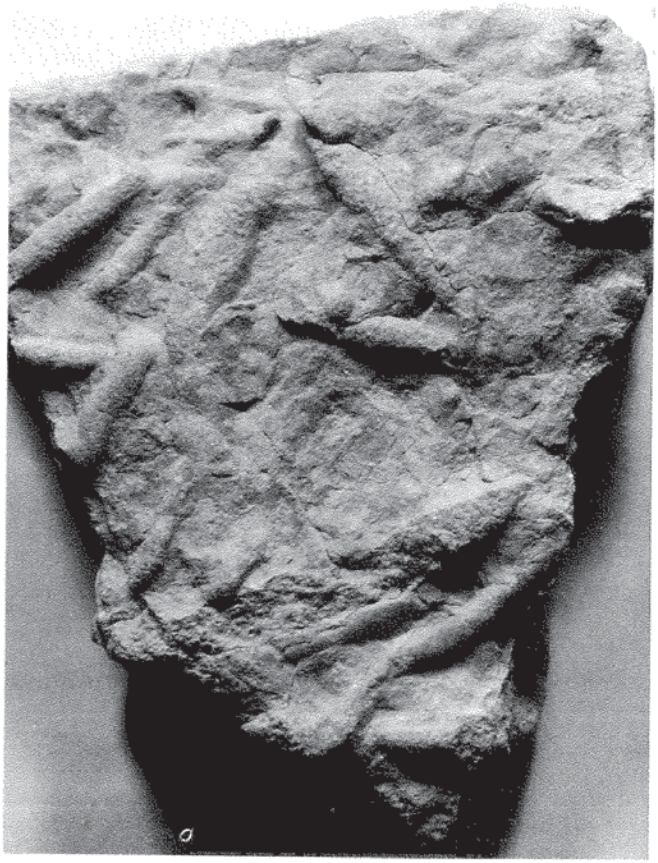

Figure 4.20

Thalassinoides burrows are complex, three-dimensional networks of traces at multiple levels, which usually collapse into a jackstraw-like web of burrows when viewed in a two-dimensional bedding plane. (Photo by D. R. Prothero.)

Zoophycos Ichnofacies

Broad, looping infaunal feeding traces known as *Zoophycos* occur in low-energy muds and muddy sands (Fig. 4.21). Traditionally, they were considered indicators of deep waters along the continental slope below storm wave base but above the continental rise where turbidites accumulate. In the standard ichnofacies scheme, this placed *Zoophycos* between the *Cruziana* and *Nereites* ichnofacies (see Fig. 4.16). However, further study has shown that *Zoophycos* can be found in a great variety of depths (Frey and Seilacher, 1980). Indeed, they appear to represent a highly versatile, opportunistic trace-maker, since they occasionally occur in the *Cruziana* and *Nereites* ichnofacies. Instead of being good depth indicators, they are more closely associated with lowered oxygen levels and abundant organic material in the sediment in quiet water settings. These conditions are indeed common on the outer shelf and continental slope, but they also occur in shallower waters of epeiric seas wherever the water is quiet enough but low in oxygen content.

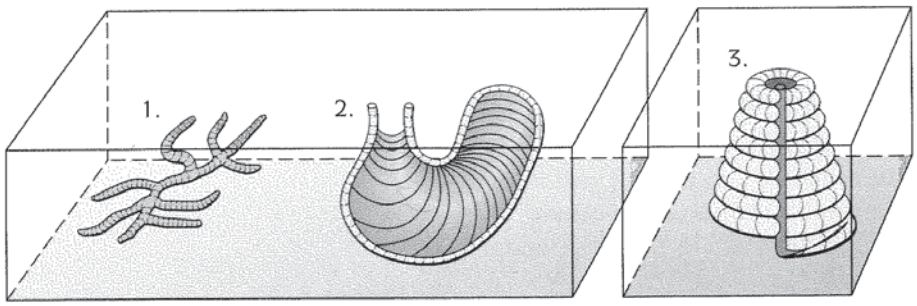

A

B

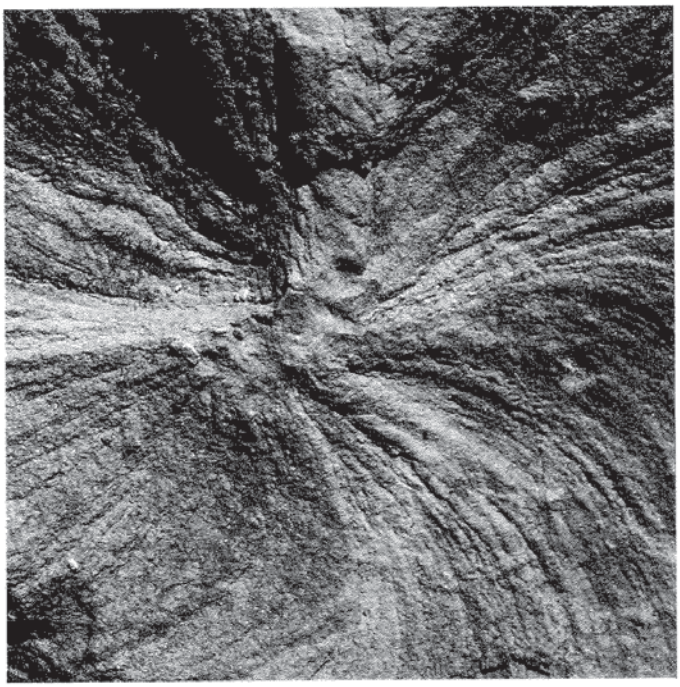

C

Figure 4.21

(A) Typical trace fossils of the *Zoophycos* facies. 1 = *Phycosiphon*; 2 = *Zoophycos*; 3 = *Spirophyton* (From Frey and Pemberton, 1984, Trace fossil facies models, in R. G. Walker, ed., *Facies Models*, pp. 189–207; by permission of the Geological Association of Canada.) (B, C) Photos of typical *Zoophycos* traces, which are a complex arcuate feeding trace in three dimensions. (B) is from the Oligocene Amuri Limestone, Vulcan Gorge, Canterbury, New Zealand; (C) is from the Eocene Saraceno Formation, Satanasso Valley, Italy. (Photos courtesy of A. A. Ekdale.)

Besides *Zoophycos*, relatively few other trace fossils are known from this community. The horizontal branched feeding trace known as *Phycosiphon* and the helically spiraling burrow known as *Spirophyton* are among the few commonly found with *Zoophycos*. The lack of diversity in the *Zoophycos* ichnofacies also suggests that it must represent a relatively hostile, oxygen-stressed environment where only a few low-oxygen-tolerant burrowers can thrive.

Nereites Ichnofacies

The interpretation of the *Nereites* ichnofacies is relatively straightforward, in contrast to that of the *Zoophycos* ichnofacies. Meandering feeding traces on bedding planes are called *Nereites* and are usually found in the abyssal plains, often associated with turbidites and deep pelagic muds (Fig. 4.22). Almost all the ichnogenera in this facies are superficial horizontal burrows in the top few centimeters of the muddy bottom. They all display some sort of regular pattern of meandering or zigzagging across the bottom, reflecting the systematic mining of the organic-rich muds of the deep seafloor for detritus.

Other Ichnofacies

Organisms can also bore their way into hard substrates. The presence of rock borings can indicate ancient shorelines and beachrock or an unconformity in which sediment was subaerially exposed. This is known as the *Trypanites* ichnofacies (see Fig. 4.16). In semiconsolidated substrates such as dewatered muds, the *Glossifungites* ichnofacies occurs. In addi-

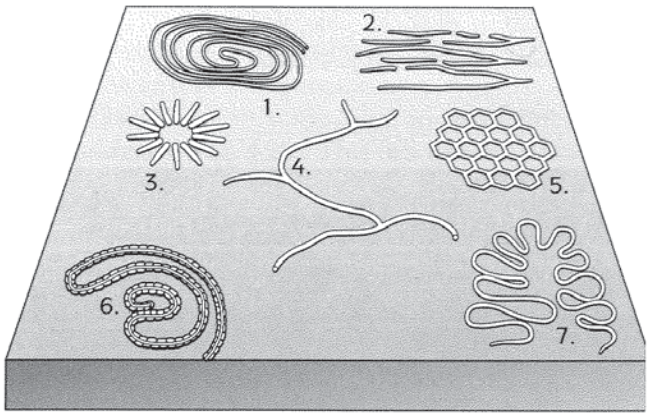

A

B

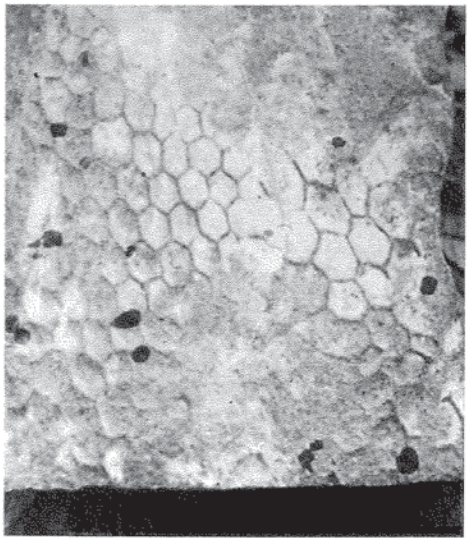

C

Figure 4.22

(A) Typical deep-water trace fossils of the *Nereites* facies. 1 = *Spirorhaphe*; 2 = *Urohelminthoida*; 3 = *Lorenzinia*; 4 = *Megagrapton*; 5 = *Paleodictyon; 6 = Nereites;* 7 = *Cosmorhaphe.* (From Frey and Pemberton, 1984, Trace fossil facies models, in R. G. Walker, ed., *Facies Models*, pp. 189–207; by permission of the Geological Association of Canada.) (B) Two different meandering traces, *Spirophycus* (larger burrows) and *Phycosiphon* (smaller burrows), Permian Oquirrh Formation, Wasatch Mountains, Utah. (Photo courtesy of A. A. Ekdale.) (C) *Paleodictyon*, a net-like trace, from the Middle Jurassic of the Ziz Valley, Morocco. (Photo courtesy of A. A. Ekdale.)

tion to a mixture of *Diplocraterion, Thalassinoides, Arenicolites,* and *Rhizocorallium,* it may also include sacklike burrows known as *Gastrochaenolites.*

The absence of trace fossils can also be informative. If there are no trace fossils in a sequence that should be heavily burrowed, there might be reason to suspect that the water was anoxic and inhospitable to organisms. In sequences that are bioturbated, individual unburrowed beds were probably deposited very rapidly, so that the organisms could rework only the uppermost part.

In summary, a working knowledge of the common ichnogenera is extremely valuable. For environmental interpretation, and especially for determining paleobathymetry and oxygen levels, ichnofossils are often the most diagnostic structures in the rock (far more definitive than the sediments themselves). Rocks with ichnofossils are much more common than those with diagnostic body fossils, so a good geologist must be ready to read the trace fossils wherever they occur.

CONCLUSIONS

When beginning geology students first examine a sandstone outcrop, all they see is rocks. The trained geologist, however, sees sedimentary structures and trace fossils and can immediately visualize the flow of the currents, the activities of organisms, and ultimately the entire environmental mosaic. As we shall see in Chapters 8–10, sedimentary structures are the most important evidence for depositional interpretations. Sedimentary structures and trace fossils are the "alphabet" that geologists use to "read" sedimentary sequences. Without them, the stones are mute.

FOR FURTHER READING

Blatt, H., G. V. Middleton, and R. C. Murray. 1980. *Origin of Sedimentary Rocks.* Prentice-Hall: Englewood Cliffs, N.J.

Bromley, R. G. 1990. *Trace Fossils, Biology and Taphonomy.* Special Topics in Palaeontology. London: Unwin and Hyman.

Collinson, J. D., and D. B. Thompson. 1982. *Sedimentary Structures.* London: Allen and Unwin.

Ekdale, A. A., R. G. Bromley, and S. G. Pemberton, eds. 1984. *Ichnology: The Use of Trace Fossils in Sedimentology and Stratigraphy.* SEPM Short Course Notes 15.

Frey, R. W., and S. G. Pemberton. 1985. Biogenic structures in outcrops and cores. I. Approaches to ichnology. *Bulletin of Canadian Petroleum Geology* 33:72–115.

Leeder, M. R. 1982. *Sedimentology, Process and Product.* London: Allen and Unwin.

Lindholm, R. C. 1987. *A Practical Approach to Sedimentology.* London: Allen and Unwin.

Pemberton, S. G., J. A. MacEachern, and R. W. Frey. 1992. Trace fossil facies models: Environmental and allostratigraphic significance. In R. G. Walker and N. P. James, eds. *Facies Models: Response to Sea Level Change.* Toronto: Geological Association of Canada.

Pettijohn, F. J., and P. E. Potter. 1964. *Atlas and Glossary of Primary Sedimentary Structures.* New York: Springer-Verlag.

Selley, R. C. 1982. *An Introduction to Sedimentology.* London: Academic Press.

Selley, R. C. 1988. *Applied Sedimentology.* San Diego: Academic Press.

Tucker, M. E. 1982. *The Field Description of Sedimentary Rocks.* Milton Keynes, England: Open University Press.